Composition, structure and dynamic properties of the Earth and planetary interiors: insights from lab experiments

Geeth Manthilake
Laboratoire Magmas et Volcans - CNRS
Universite Clermont Auvergne
Clermont Ferrand

Laboratoire Magmas et Volcans
Clermont Ferrand, France

1. Introduction

Earth's evolution from a fire-ball state to a habitable planet

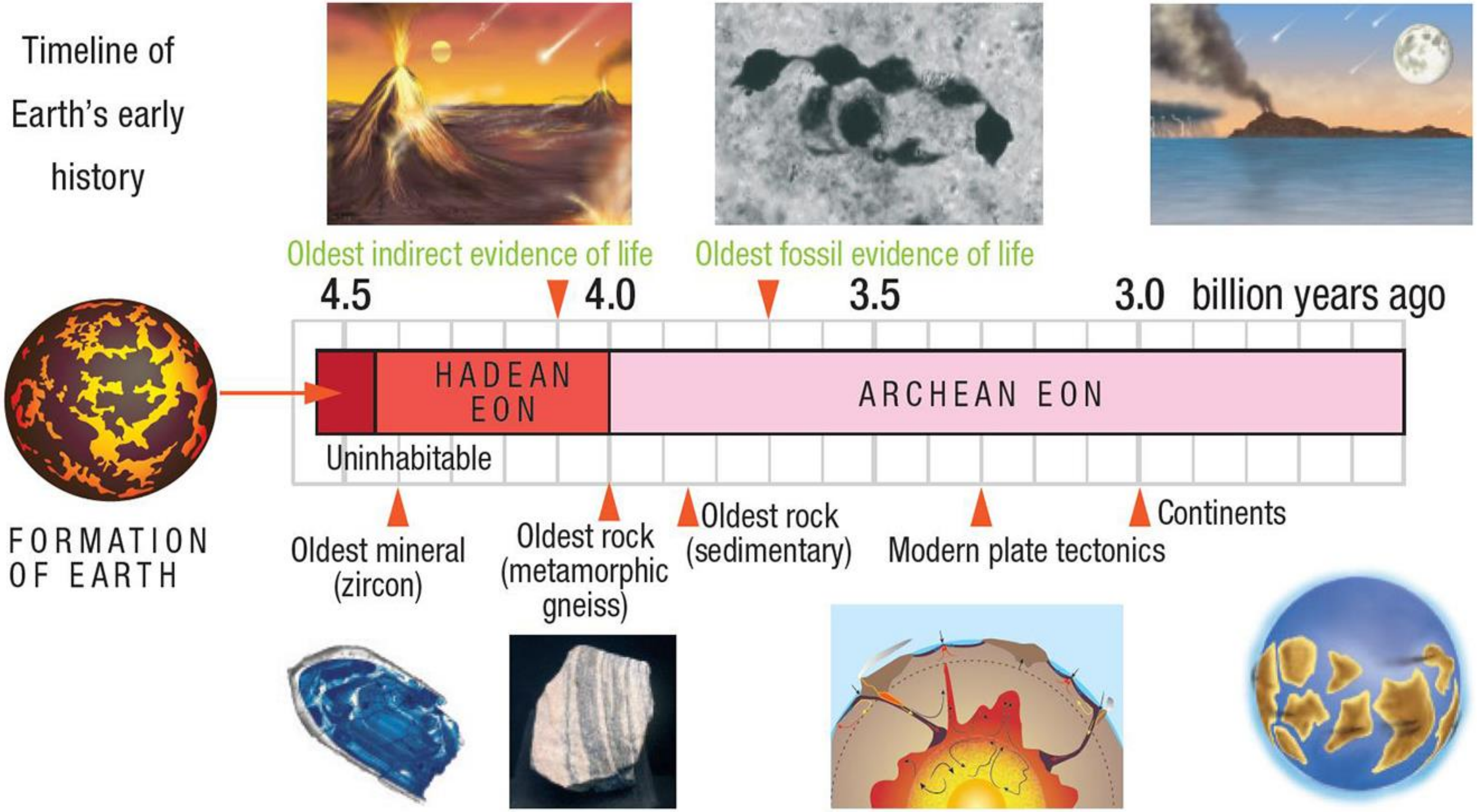

Early Earth

- Formation of the metallic core
- Magma ocean crystallization
- Solidification of the inner core
- Compositional stratification

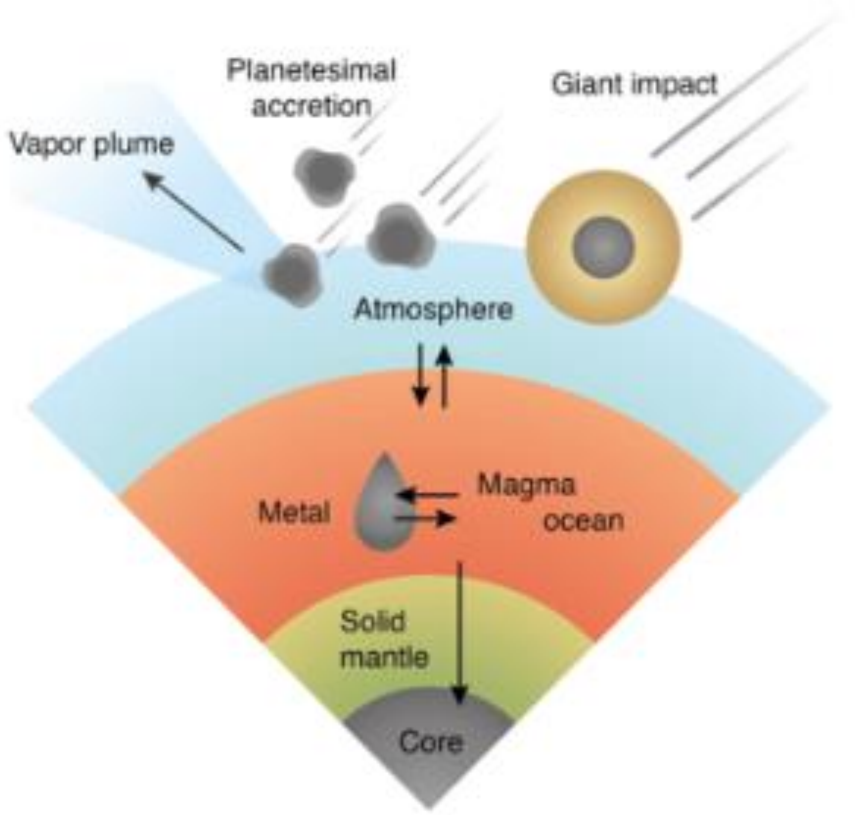

Source: TITEC

Present-day Earth

Electrical resistivity

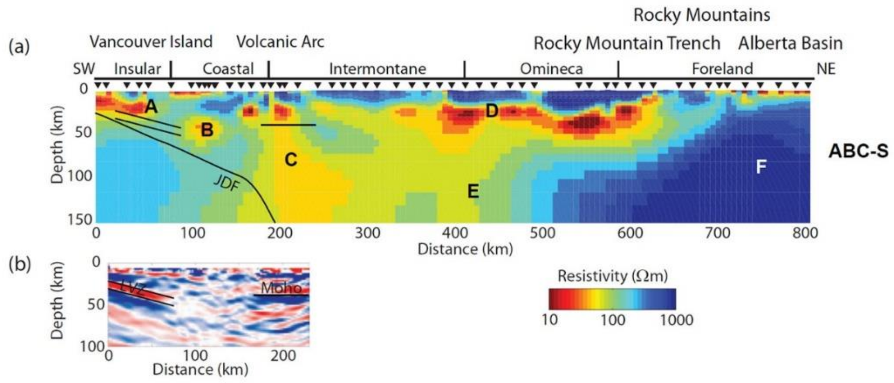

Seismic wave velocity

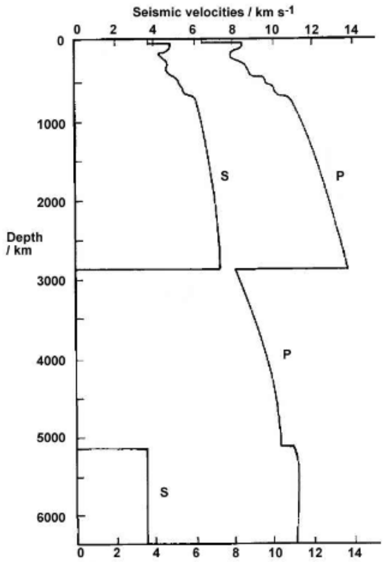

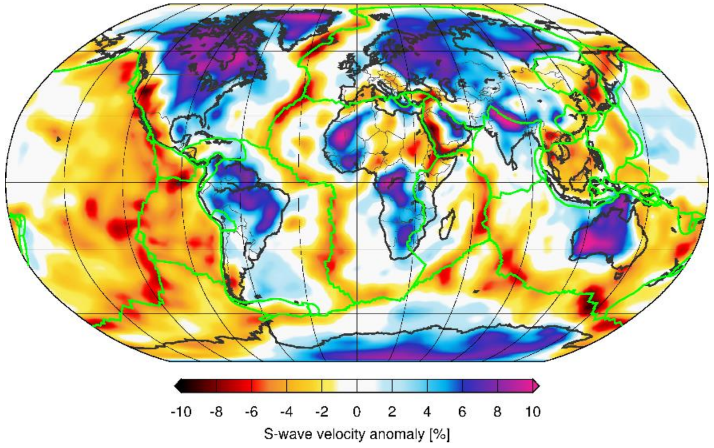

Heat flow

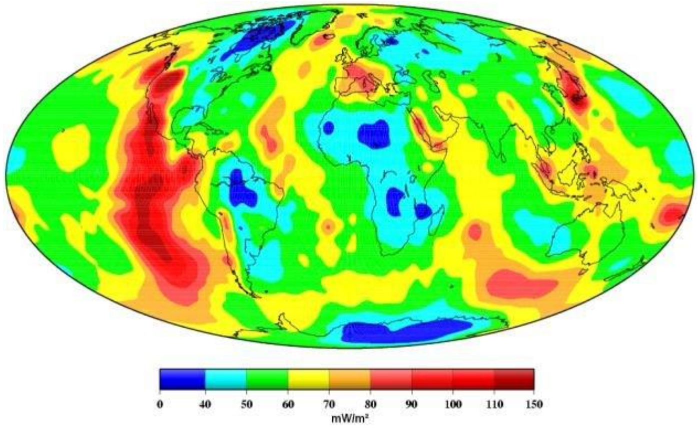

Geophysical profiles represent variation in

- temperature
- composition
- density
- physical state

Source: Institute of Physics

2. Applications

- Material circulation
- Mantle heterogeneities
- Heat transport in the Earth and Planetary bodies

- Transport of water into the lower mantle
  - High water contents (2 wt. %) in OIBs fed by plumes rising from the LM (Deschamps et al. 2011)
  - Continental sediment components in OIBs (Hart 1988) - EM-II

- K-hollandite (liebermannite):
  - principal phase in continental sediments (30 vol. %),
  - K-rich MORB
- Stable from the crust to core
  - K-feld – K-Hol (low P) – K-Hol (High P)
- tunnel structure – a repository for incompatible cations
- possible water carrier

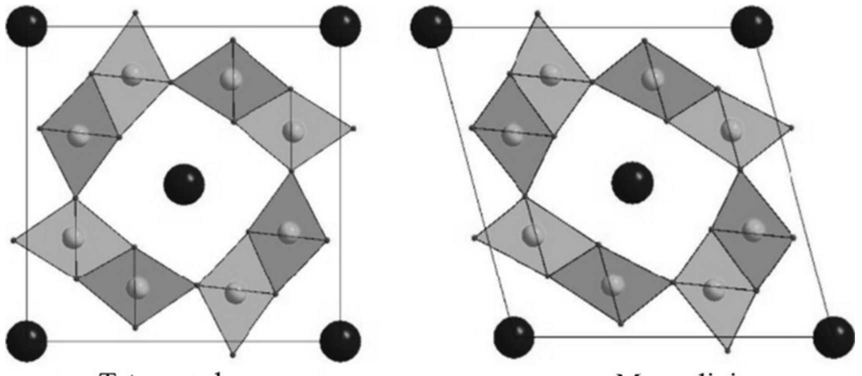

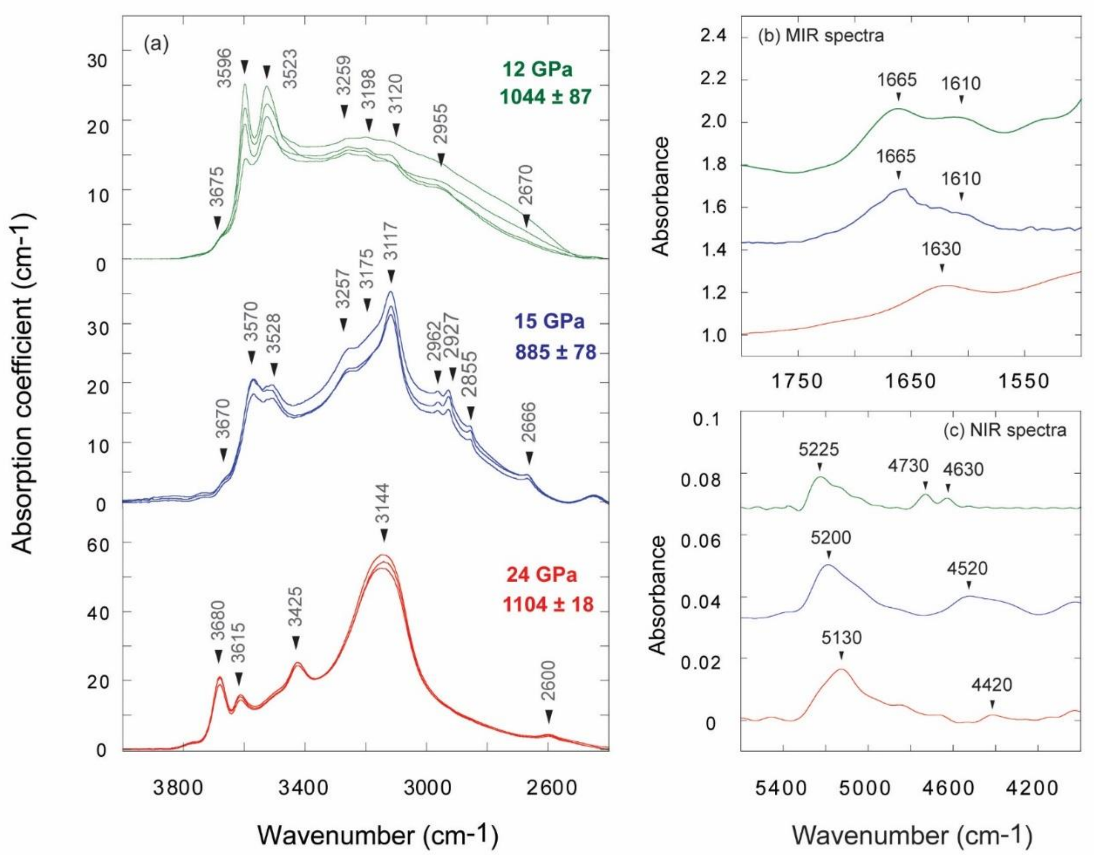

Manthilake et al. 2019

K-hollandite- A super ionic conductor

Superionic conduction : fast motion of K^+ or H^+ in the tunnel

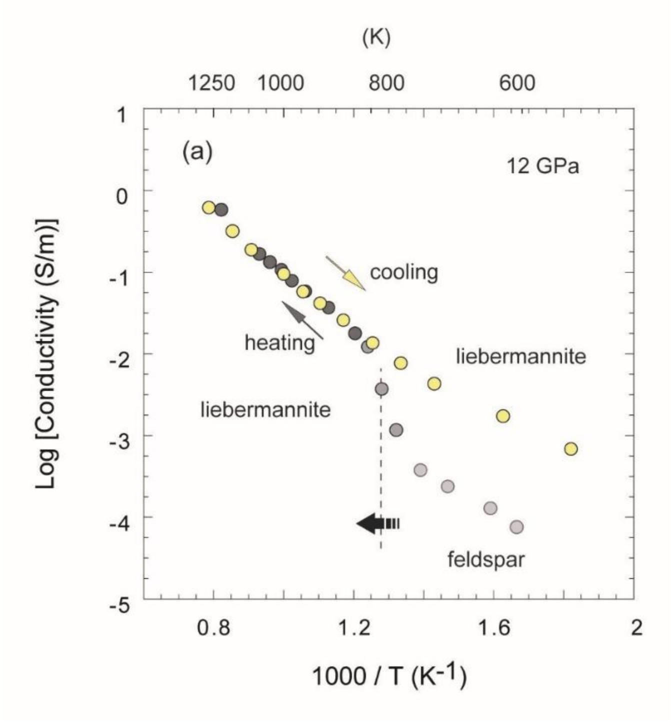

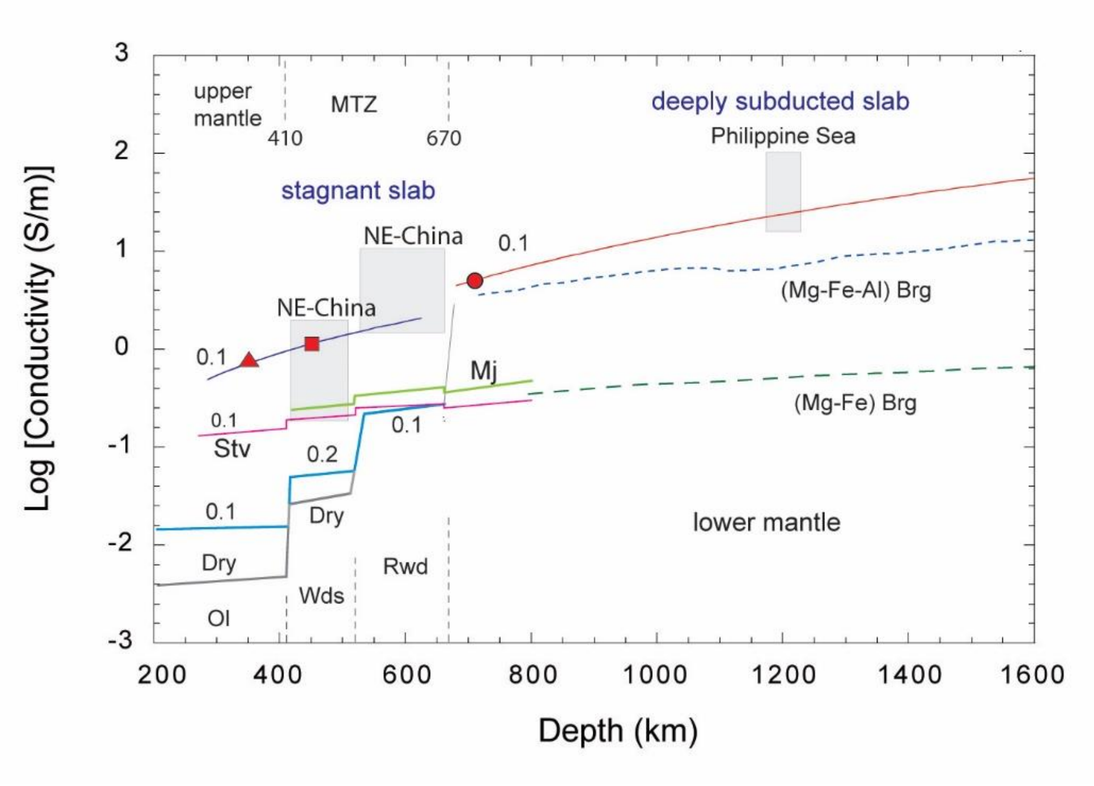

Tracer mineral for subduction pathways of continental sediments

Manthilake et al. 2019

Water in the Earth's upper mantle

- The earth's upper mantle contains 50-200 et. ppm water

diffusion

Mantle upwelling

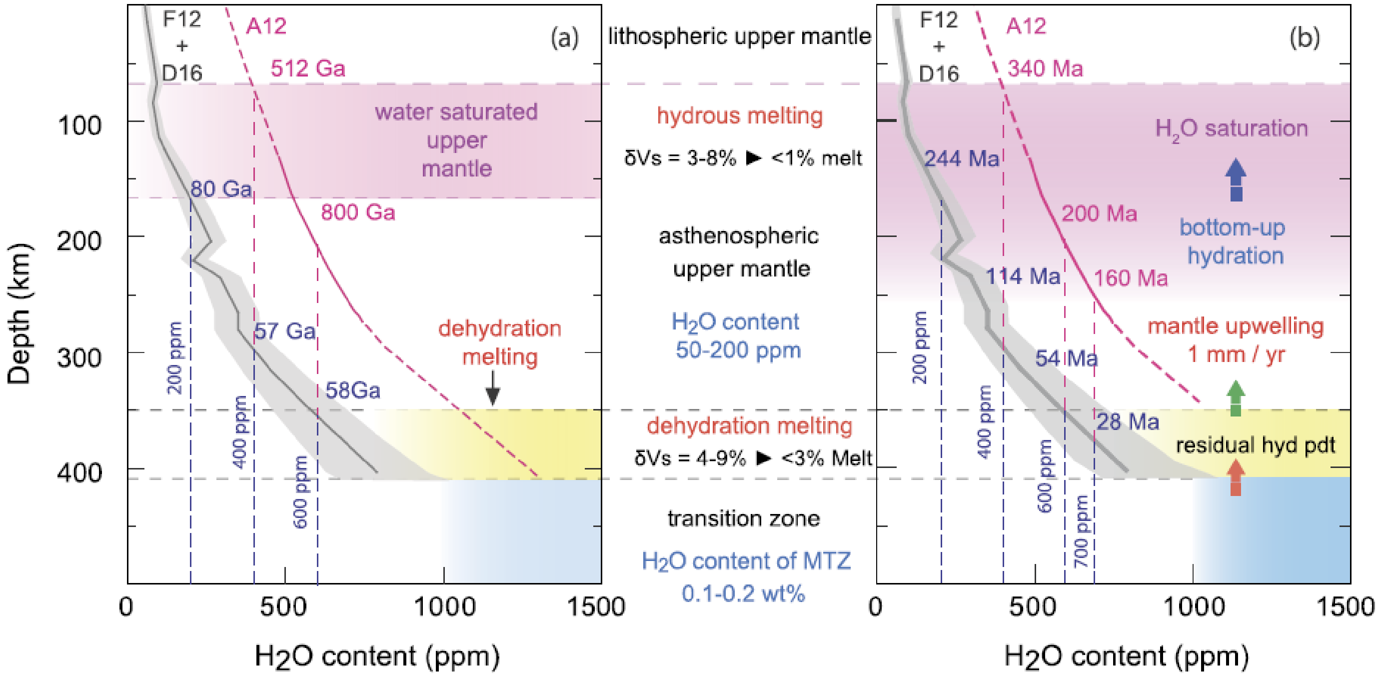

$$\frac{c_x - c_0}{c_s - c_0} = 1 - \mathrm{erf}\left(\frac{x}{2\sqrt{Dt}}\right)$$

C_s = Concentration of source
C_x = Concentration at distance x
C_0 = Concentration of h0st

Freitas and Manthilake et al. 2019

Conductivity profile of the upper mantle

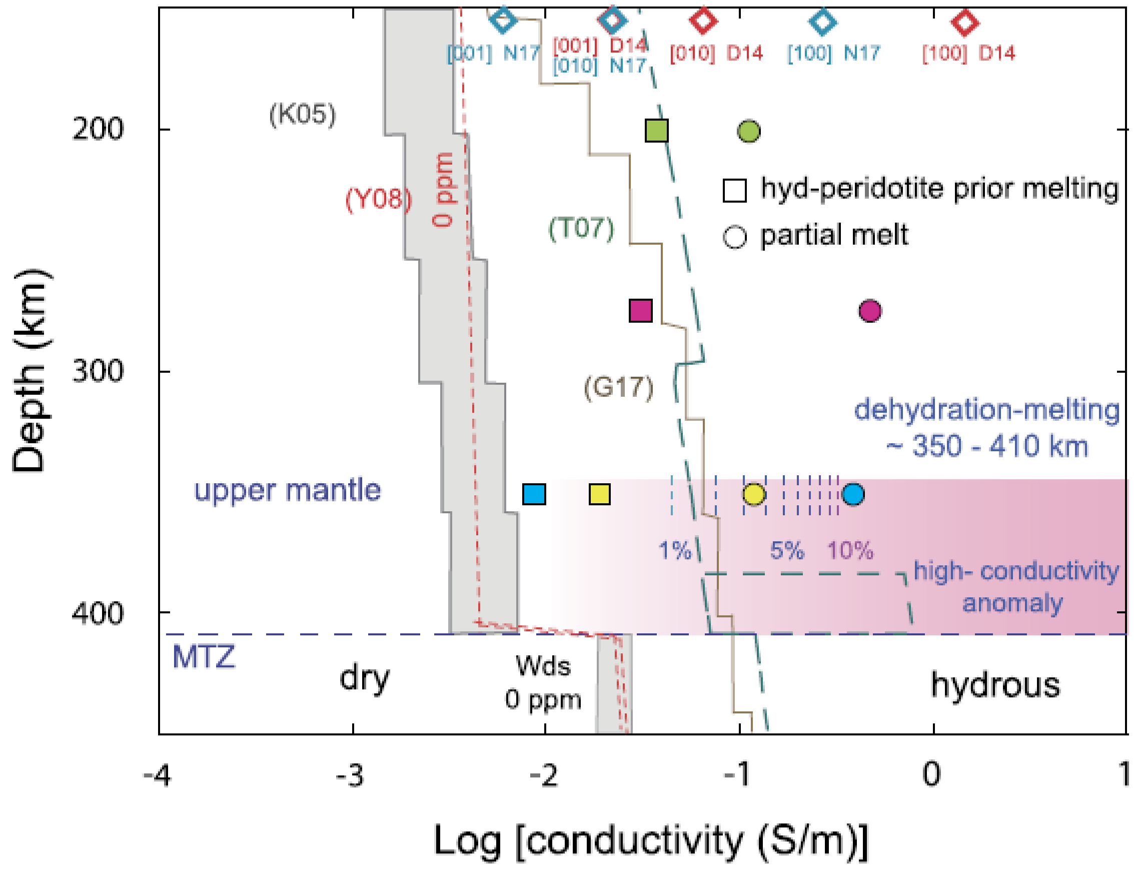

Freitas and Manthilake et al. 2019

Physical properties of fluids

- Dehydration of hydrous phases releases aqueous fluids into the mantle wedge
  - Affect the oxidation conditions
  - Mantle flow
  - carrier for the trace elements

Wetting properties

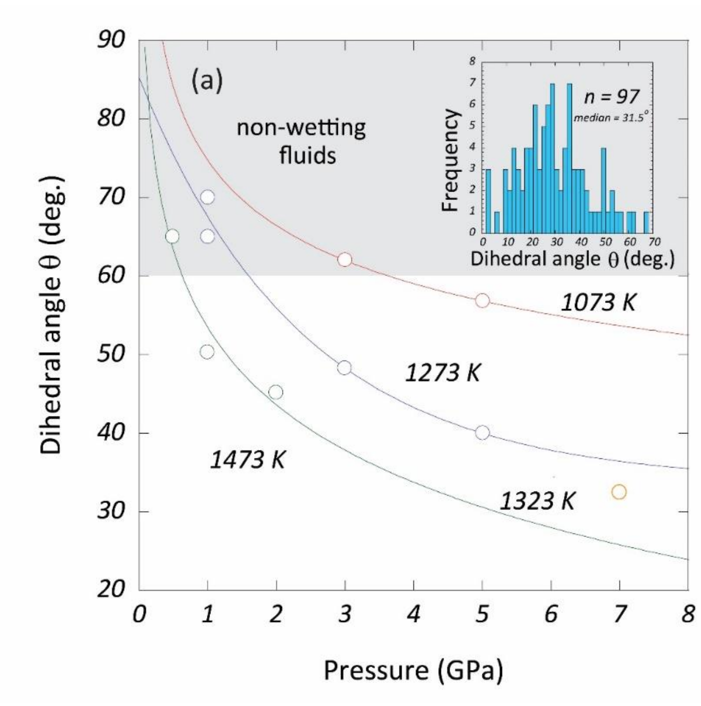

Electrical properties

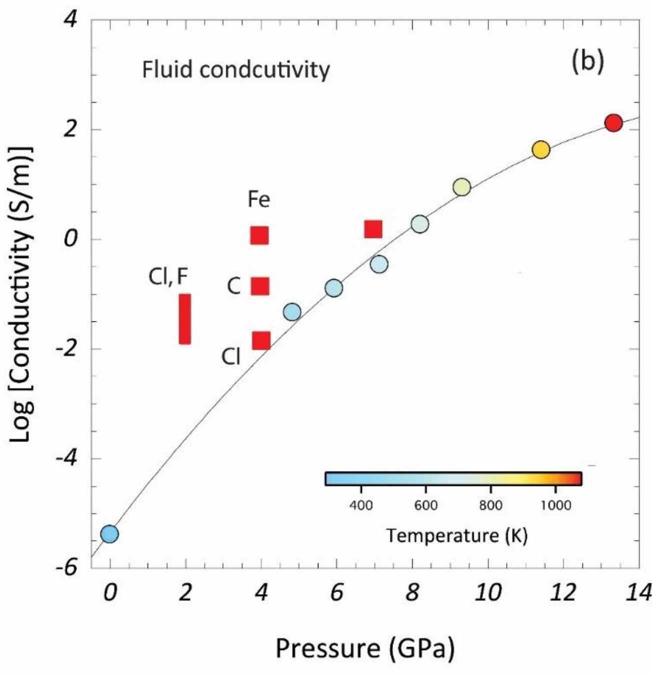

Seismic properties

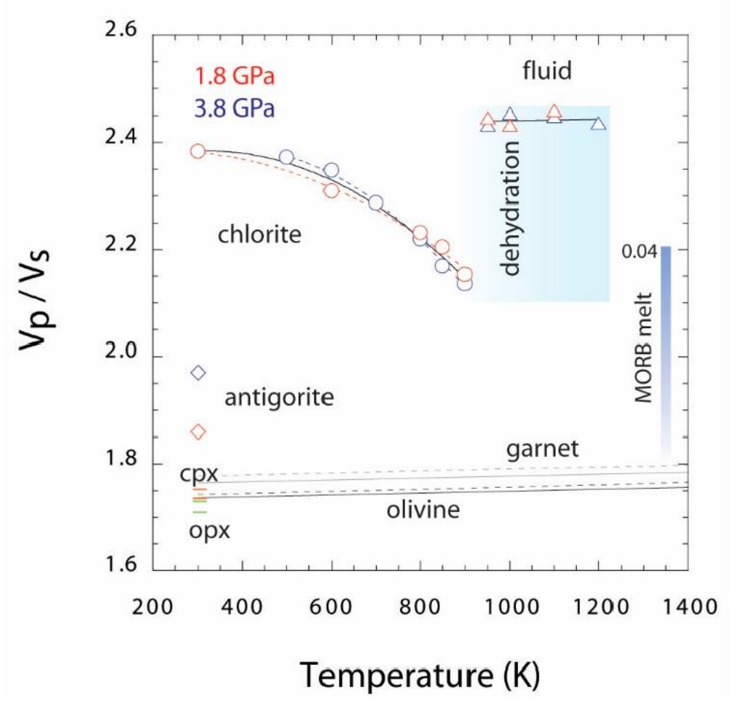

Manthilake et al. 2015,2016,2021a, 2021b   Mibe et al. 1999

Fluid in subduction zones

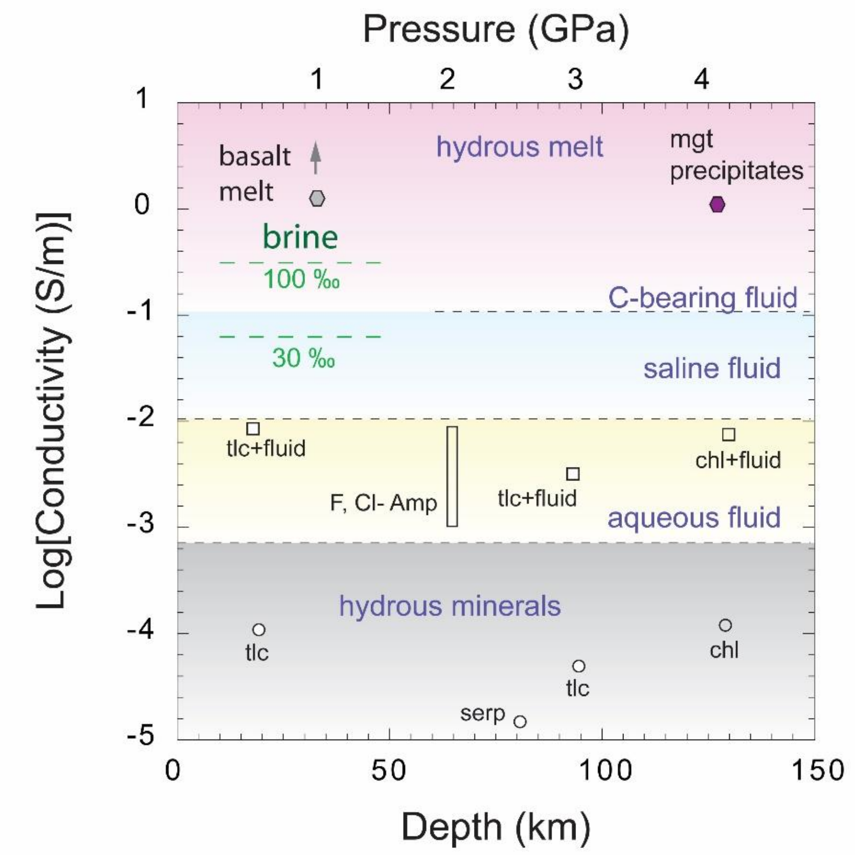

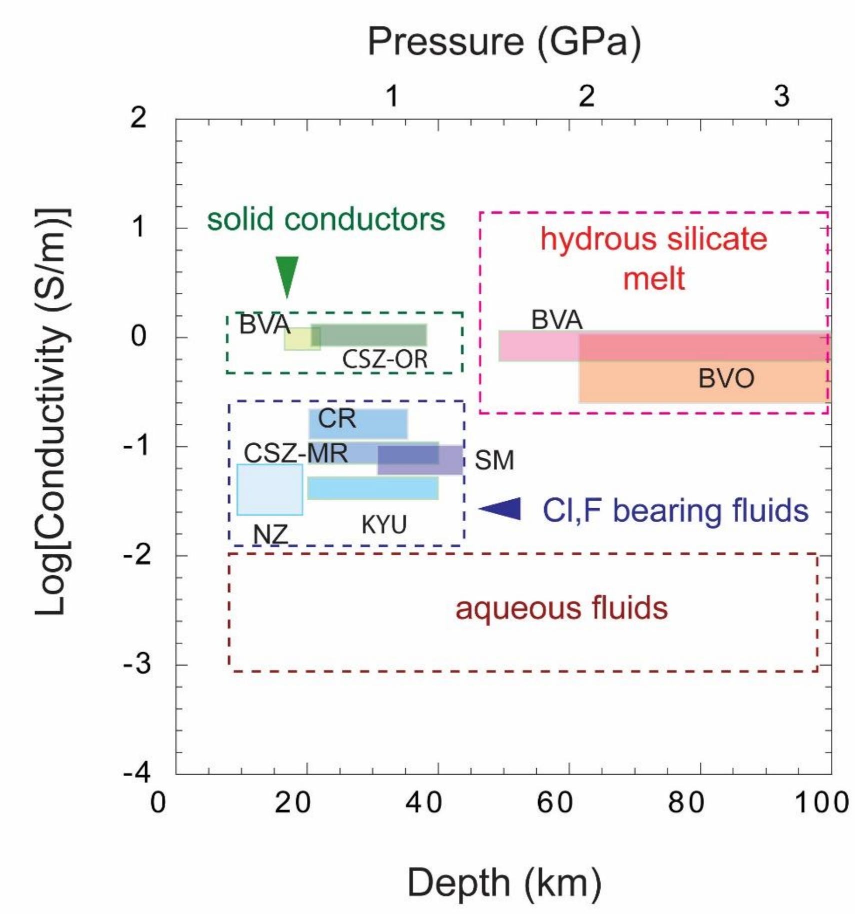

Manthilake et al. 2015,2016,2021a, 2021b

Electrical conductivity as a geothermometer

- Slab surface temperature – stability of minerals, melting, deeply subducting slab
- A numerical model based on finite element analyses (e.g. Syracuse et. al 2011)

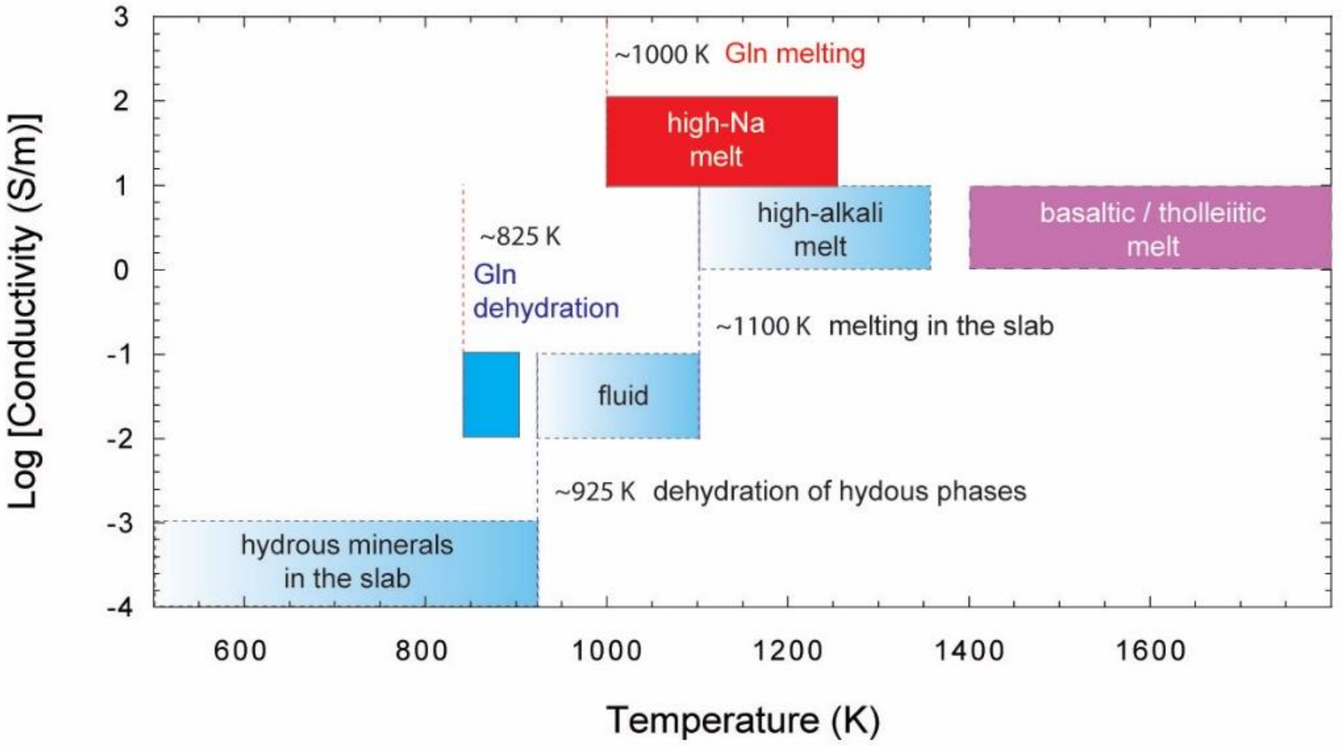

Manthilake et al. 2021

Application to NE-Japan subduction system

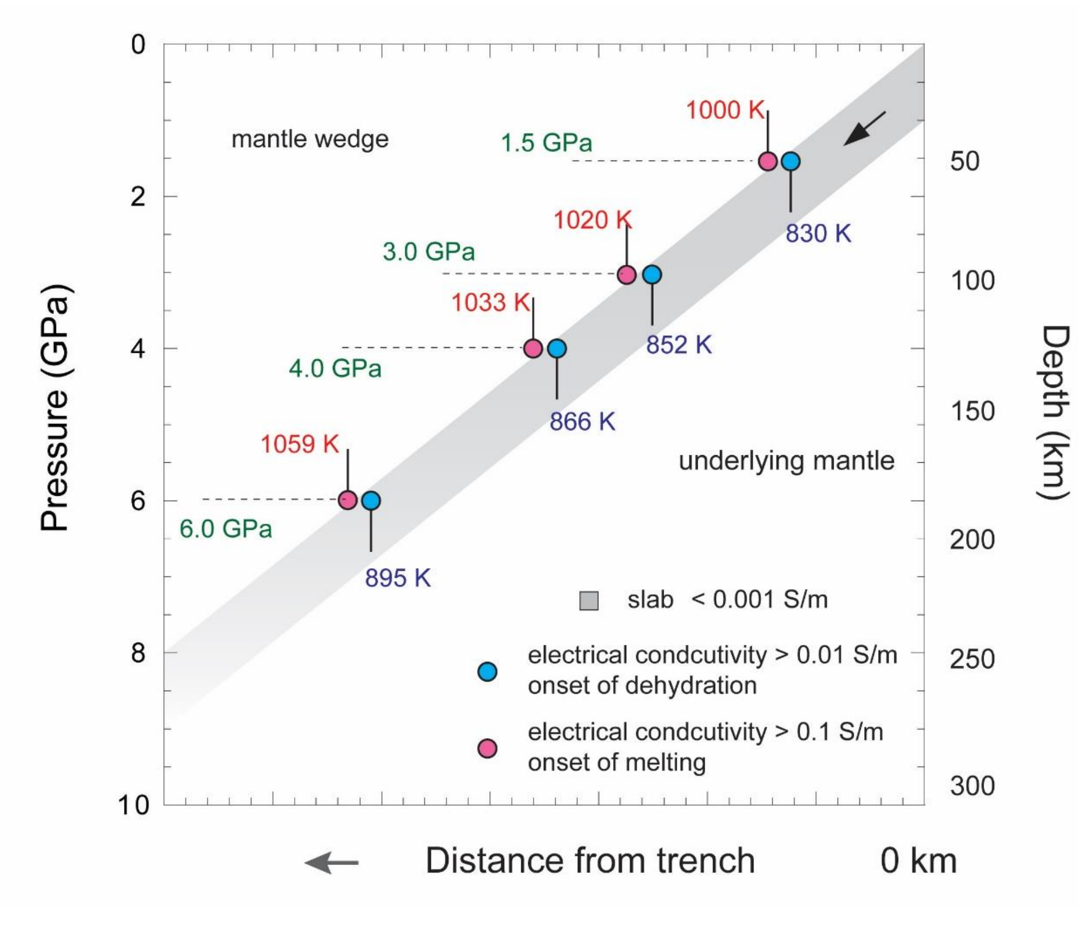

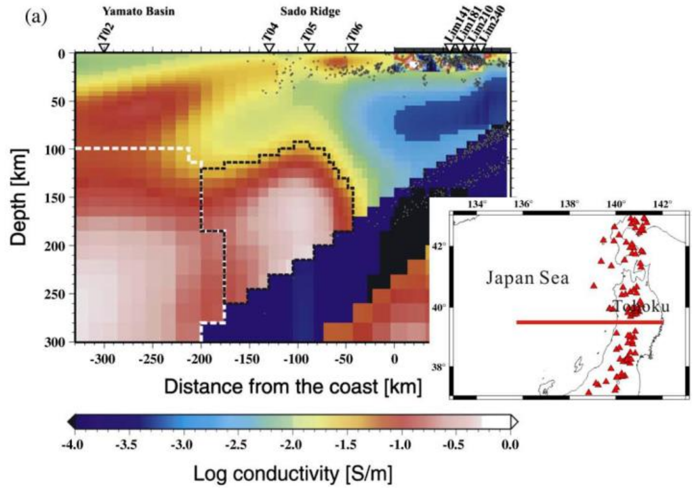

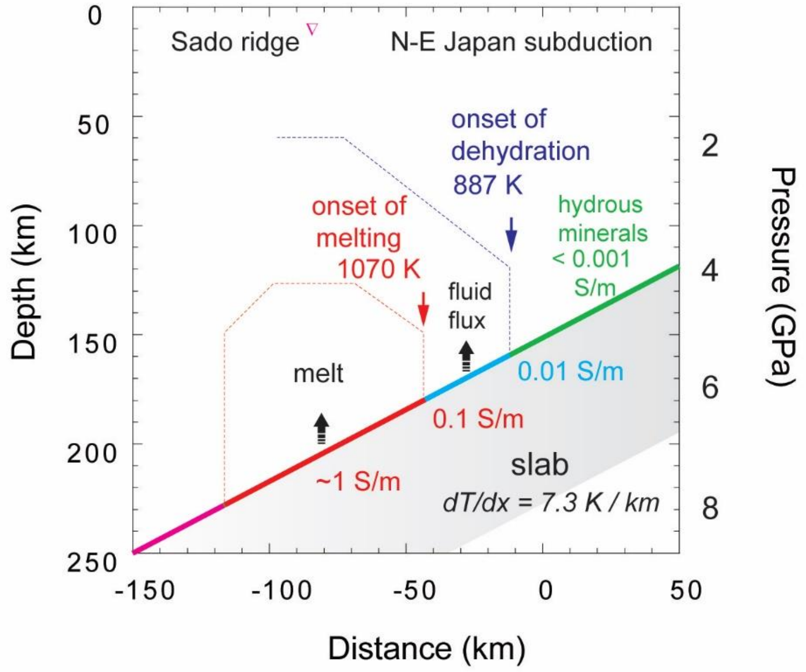

Manthilake et al. 2021

Recycling of carbon through subduction

- The decarbonation and dehydration in subduction zones are intricately related.
  Most studies evaluate them separately

- Physical properties of CHO fluids
- carbon circulation in the mantle wedge
- the mechanisms of deep carbon subduction

Starting materials:
Carbonate-bearing chrysotile

HP-HT Experiments :
4 GPa and up to 975 K

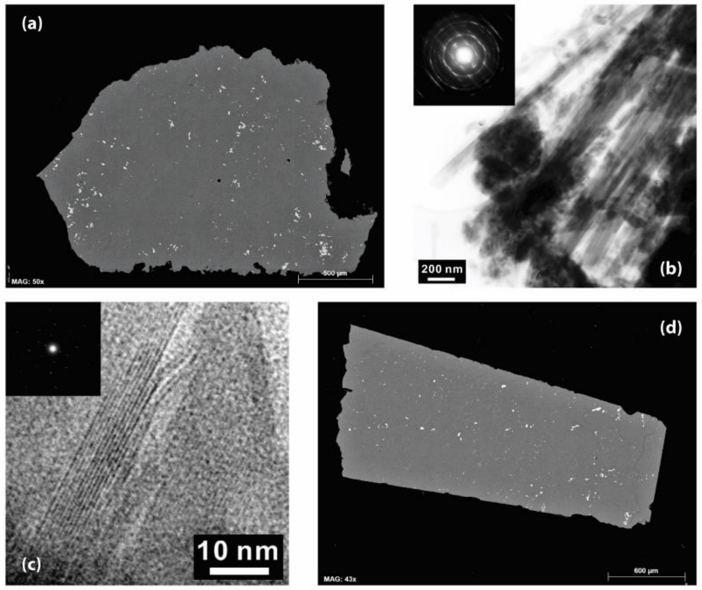

Manthilake et al. 2021

Recycling of carbon through subduction

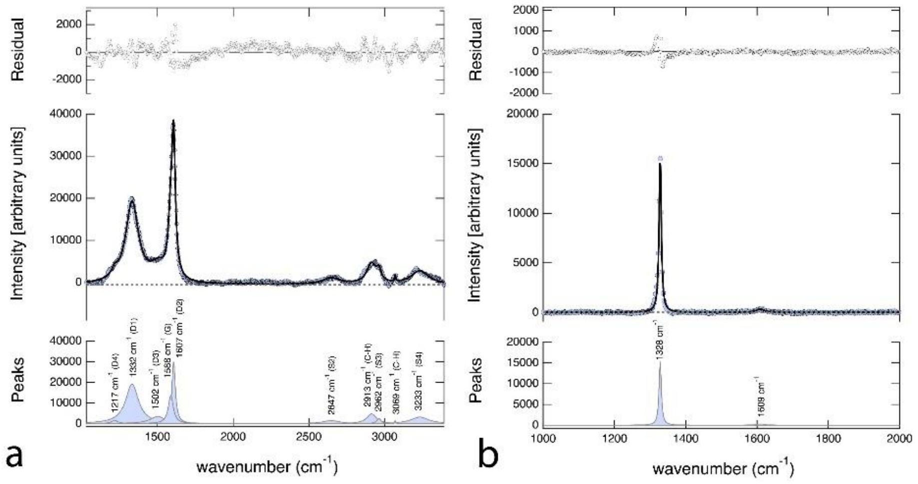

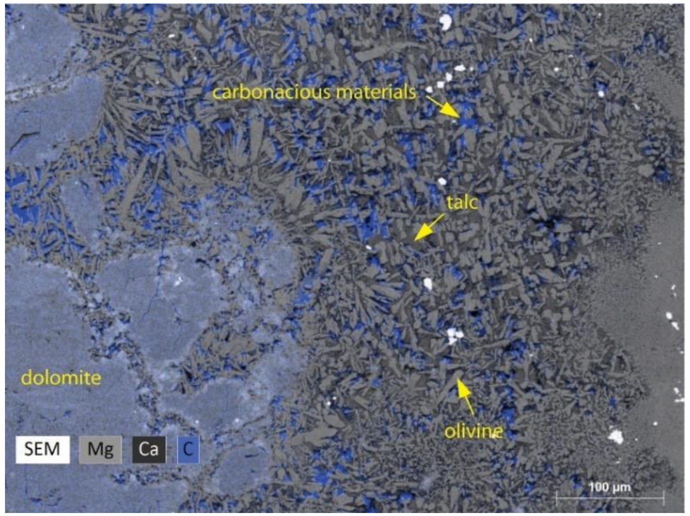

Manthilake et al. 2021

- The presence of carbonaceous materials suggests the following reactions
  $CO_2 = C + O_2$,
  $CO_2 + 2H_2O = CH_4 + 2O_2$
- The presence of diamonds at low T suggests the reactions:
  $CH_4 = C + 2H_2$
  $CH_4 + O_2 = C+2H_2O$
- Supports the formation of subduction-related micro-diamonds in ultrahigh-pressure metamorphic terrains
- Crystallization of dolomite could be a key process responsible for transporting carbon into the deep Earth

Large-scale mantle structures

- Partial melt layer atop the mantle transition zone

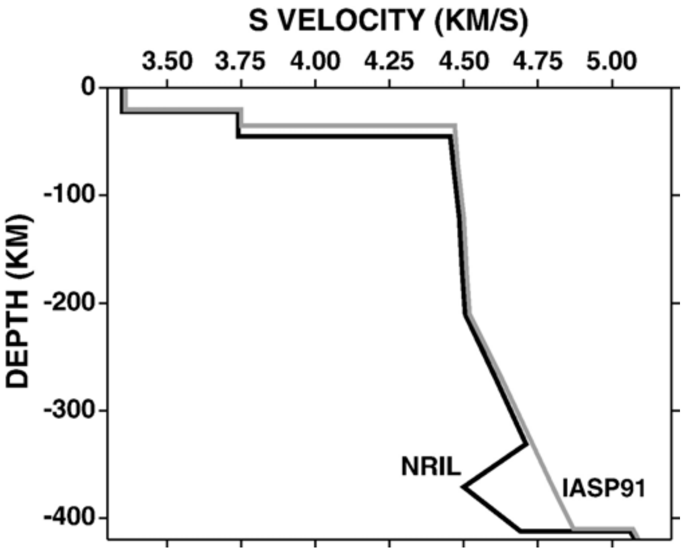

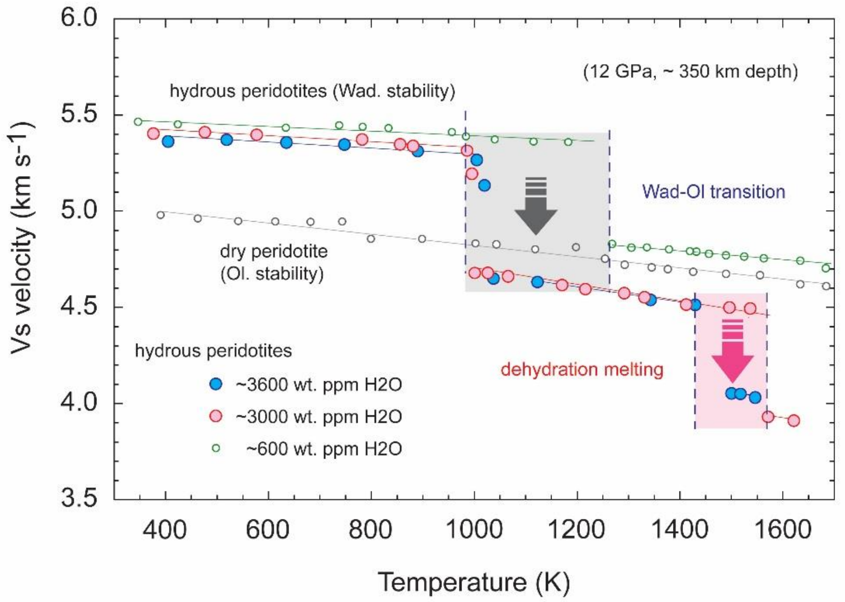

1[st] Vs drop - Wad to Ol transition

2[nd] Vs drop - melting

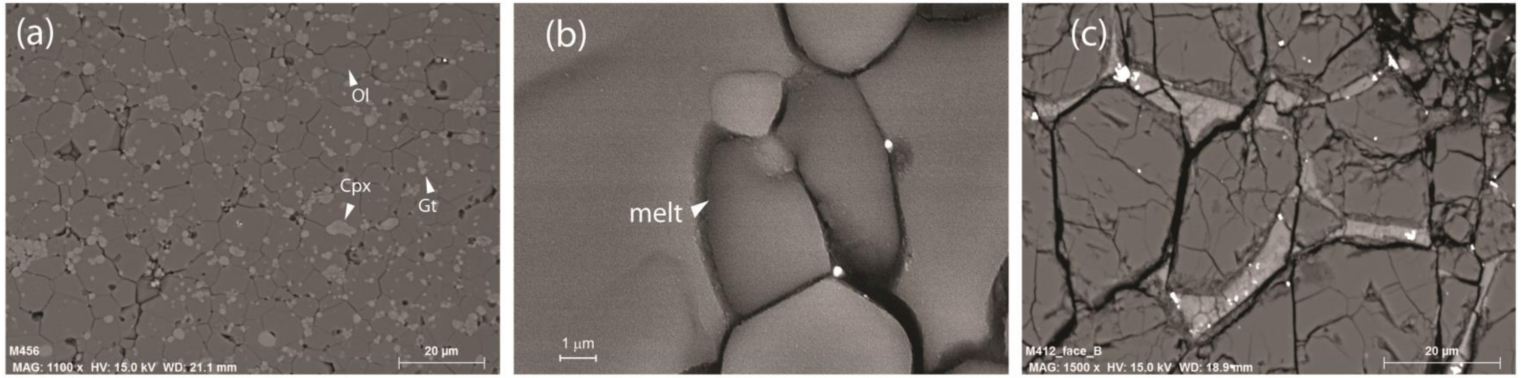

Freitas et al. 2017

Large-scale mantle structures

- Stable melt layer atop the mantle transition zone

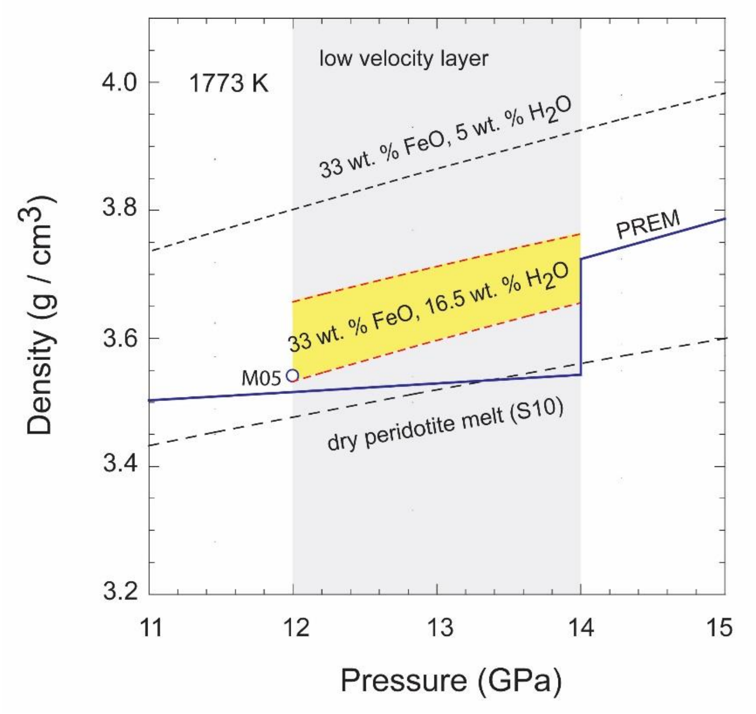

- The density of melt 3.56- 3.74 g cm^{-1}
- Neutrally buoyant at 350-410 km depth
- 4 % shear velocity drop: compatible with 0.7 - 1.0% melt
- MTZ water contents ~ 0.22 ± 0.02 wt. %
- MTZ is water undersaturated

Freitas et al. 2017

Large-scale mantle structures

- Deformation of Ol+Opx mixtures in upper mantle conditions

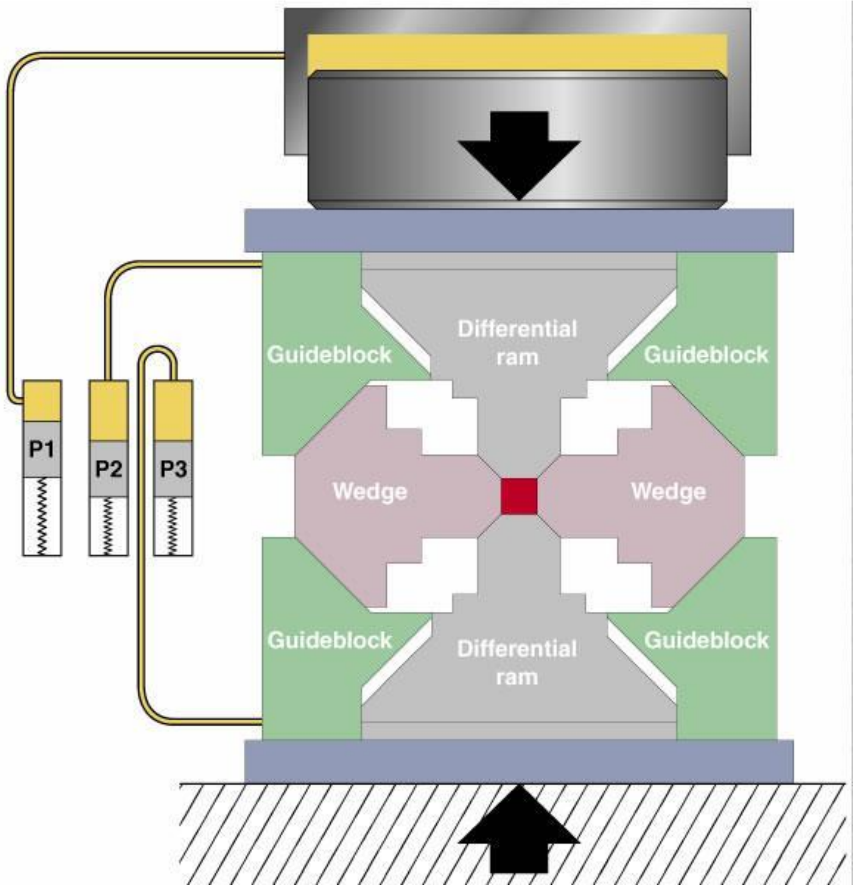

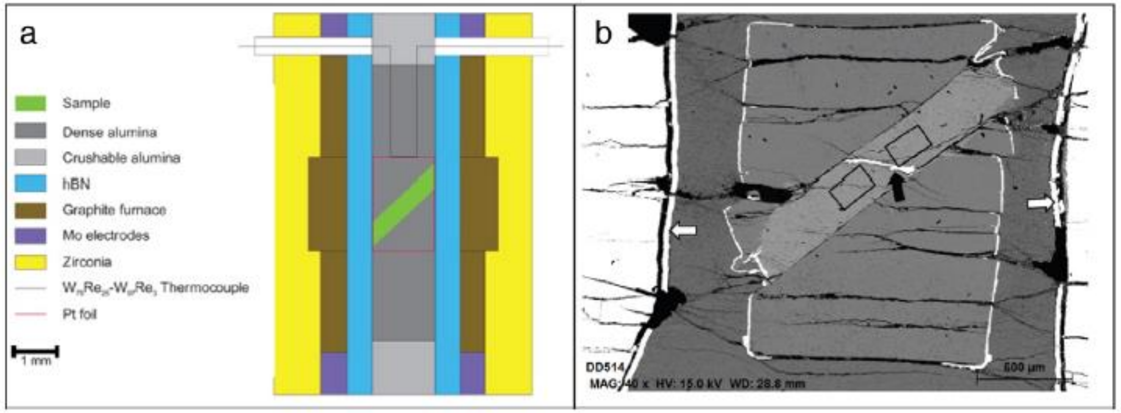

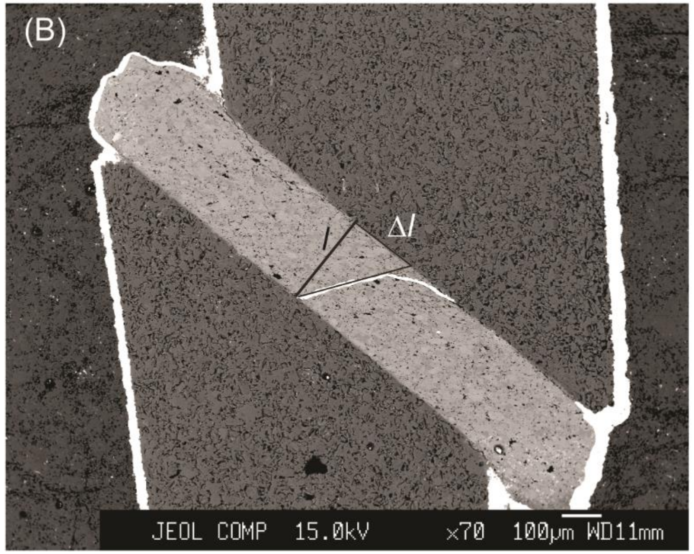

Soustelle and Manthilake 2017

Large-scale mantle structures

- Deformation of Ol+Opx mixtures

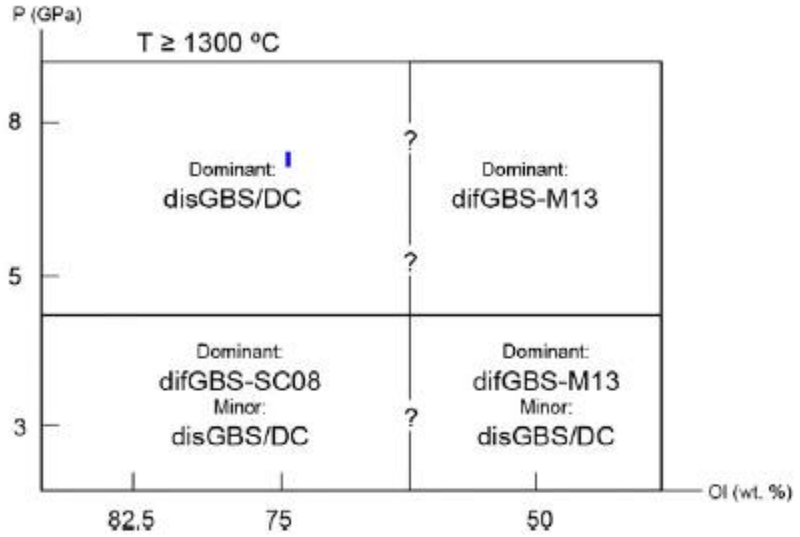

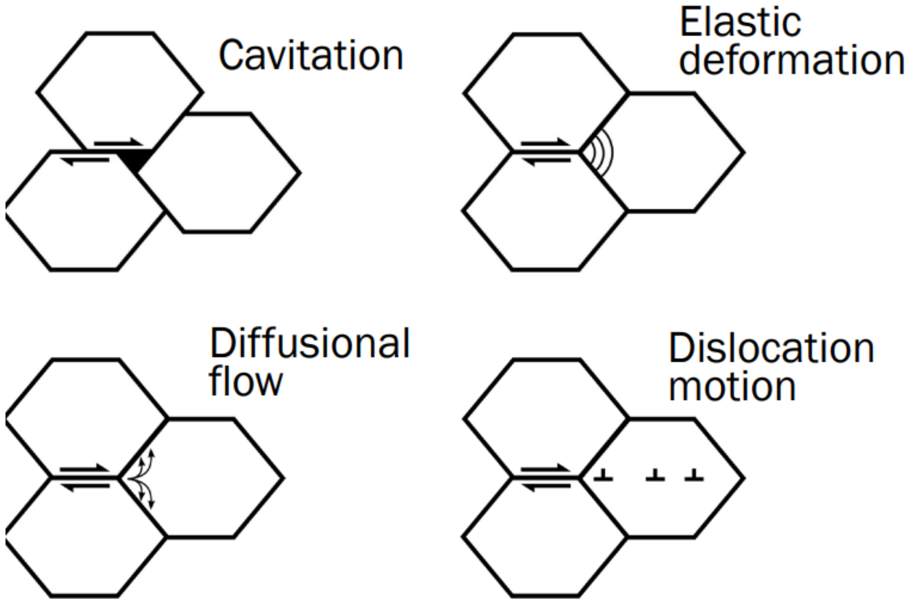

diaGBS – dislocation-accommodated grain boundary sliding
difGBS – diffusion-accommodated grain boundary sliding

Soustelle and Manthilake 2017

Planetary heat transport

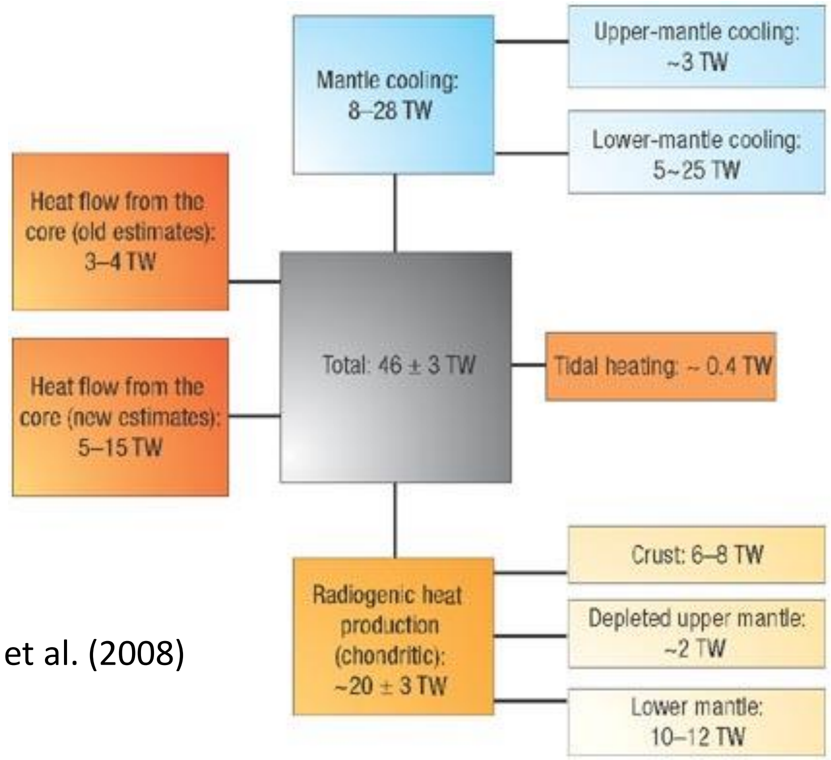

Lay et al. (2008)

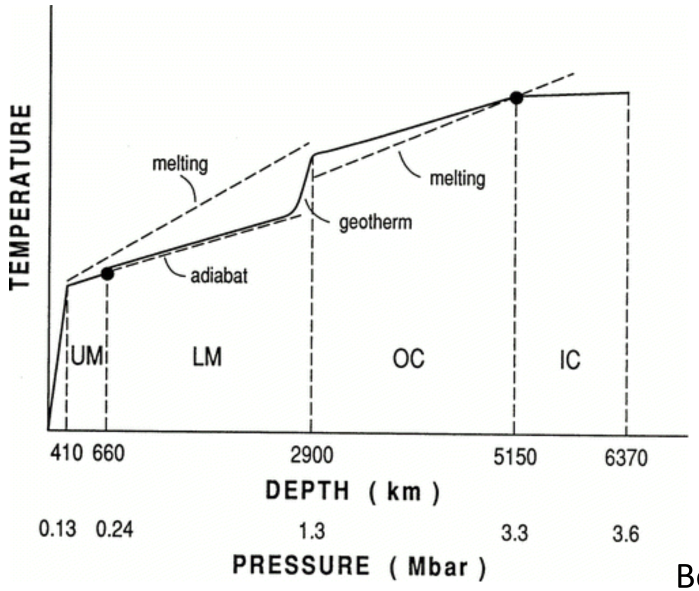

Boehler (1996)

- Heat flows through TBL via conduction

Key parameters

–Thermal conductivity

–Temperature

–Thickness of TBL

$$\frac{\Delta Q}{\Delta t} = -\kappa A \frac{\Delta T}{\Delta x}$$

Pressure and temperature dependence TC of brigmanite

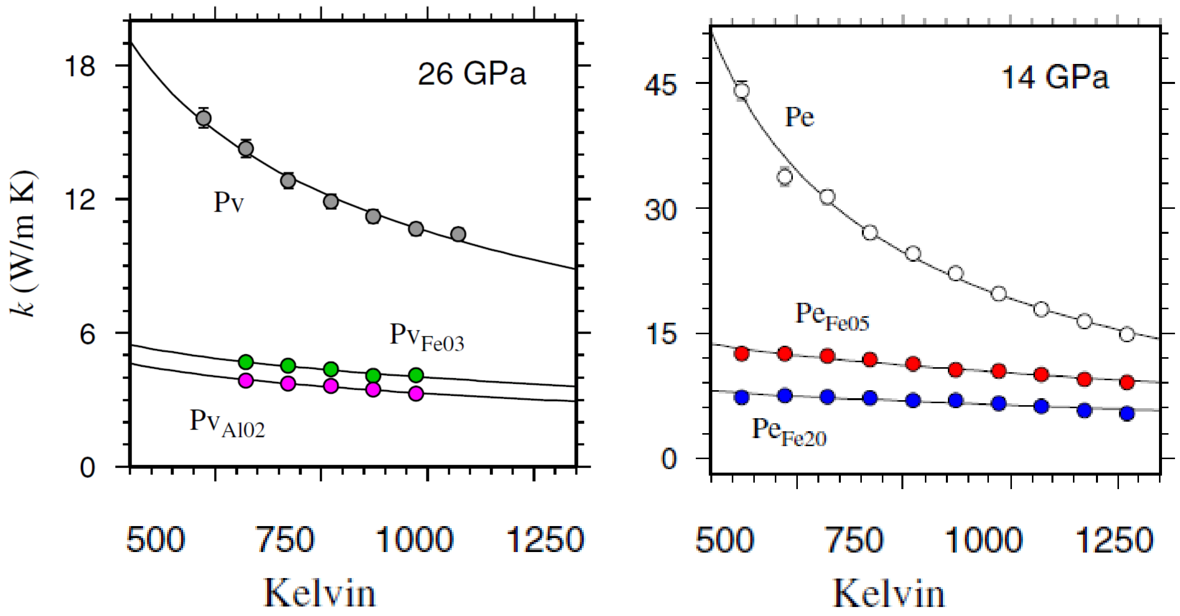

$$\kappa = \kappa_{ref}\left(\frac{T_{ref}}{T}\right)^{a}\left(\frac{\rho}{\rho_{ref}}\right)^{g}$$

Effect of impurities – incorporation of Fe, Al decrease the κ by 50 %

Manthilake et al. 2011a, 2011b

Core-mantle boundary heat flux

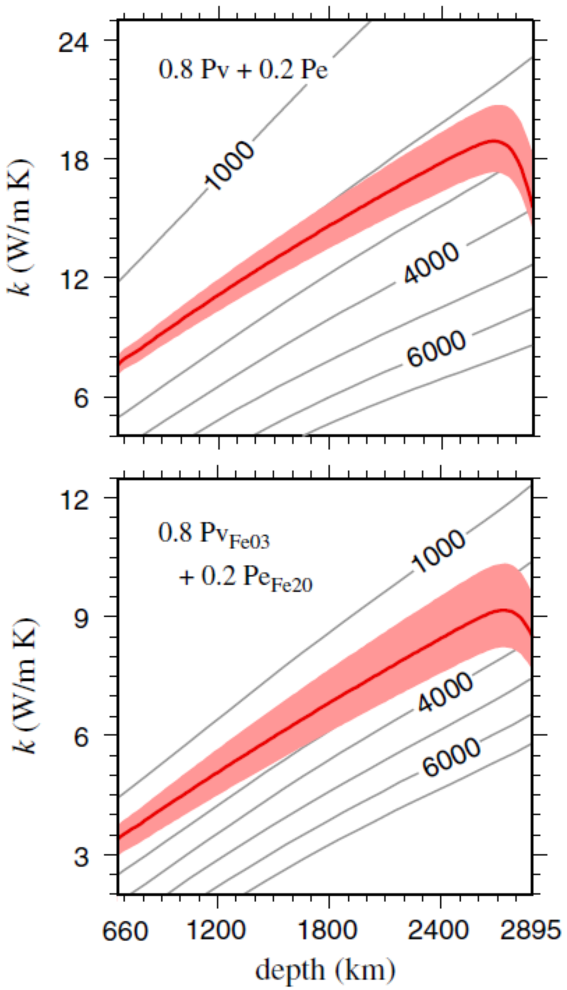

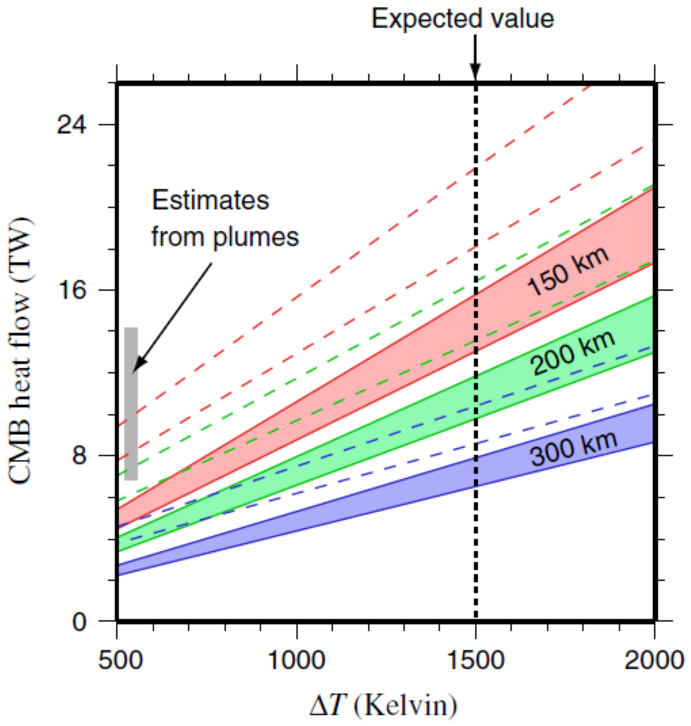

pure MgO-MgSiO3 aggregate
of 18.9-15.4 W/ m K

lattice thermal conductivity at TBL
8-9 W/ m K

CMB heat flow 11±1.4 TW

Manthilake et al. 2011a

Towards a comprehensive core-mantle boundary heat flow model

- Thermal conductivity of constituent phases along and across the TBL

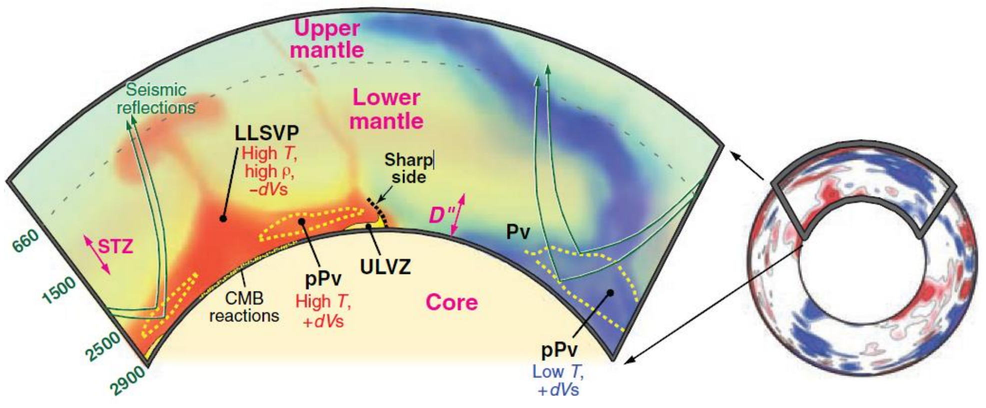

Garnero and McNamara (2008)

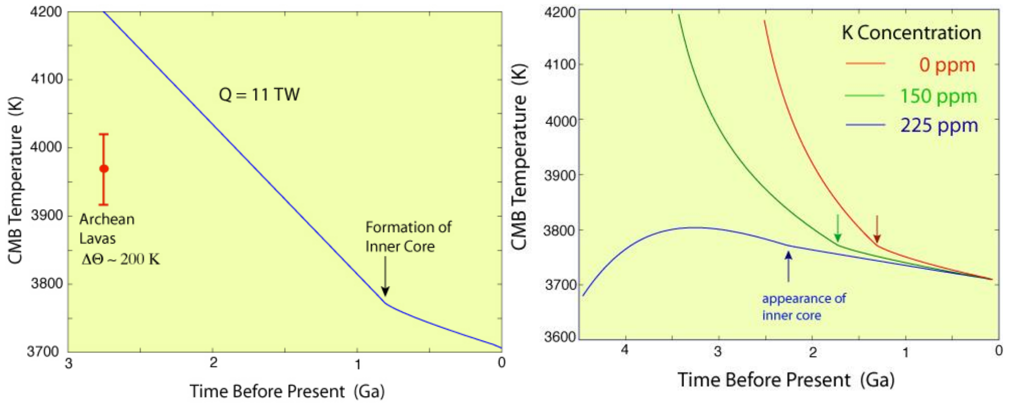

Buffett 1994

According to seismology, CMB may consist of a mixture of

- Brg, Fp and PPv
- Subducted materials (MORB)
- Core reactant products,
- Partial melt, metallic alloys

- Thermal instabilities at the CMB
  - Formation of mantle plumes
- Evolution of the TBL/heat flow with time
  - Sets the age of the inner core
- constrains the radiogenic isotopes budget in the core/CMB

A comprehensive core-mantle boundary heat flow model

- The work in progress

Characterization of thermal conductivity of a melt bearing system

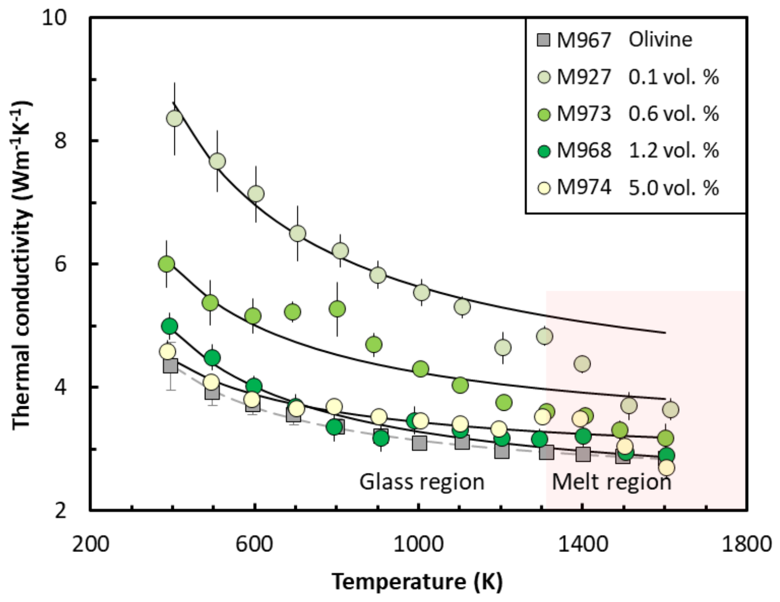

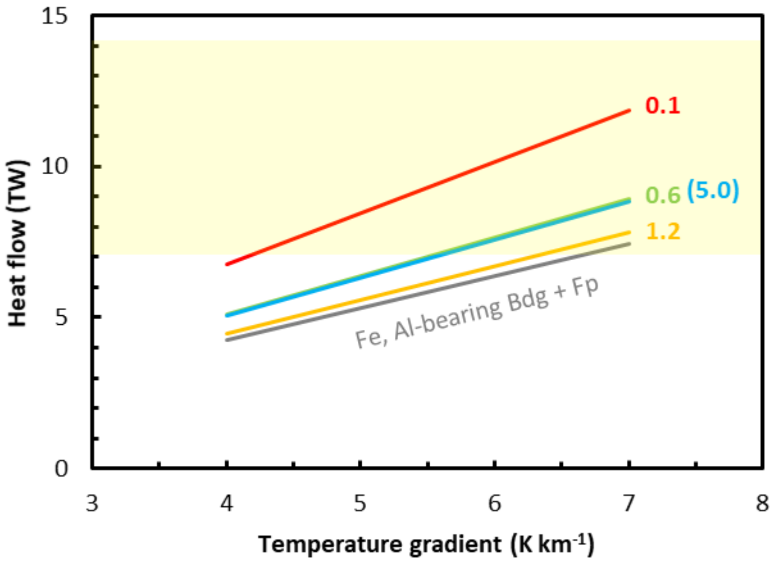

Zhao et al. in prep

Thermal evolution of the planet Mercury

- Thermal conductivity of Fe-S alloys

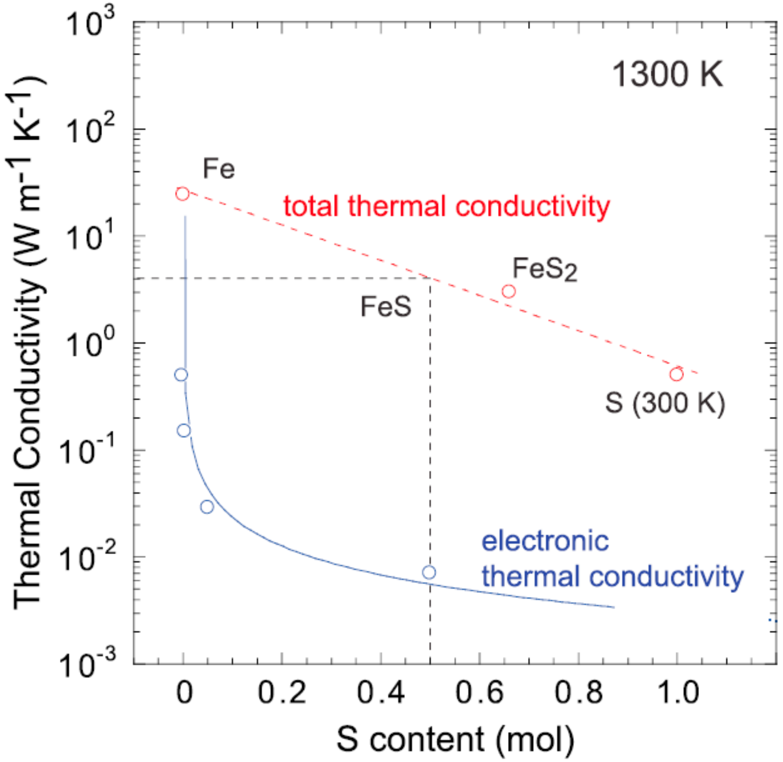

Calculated heat flow at Mercury’s CMB

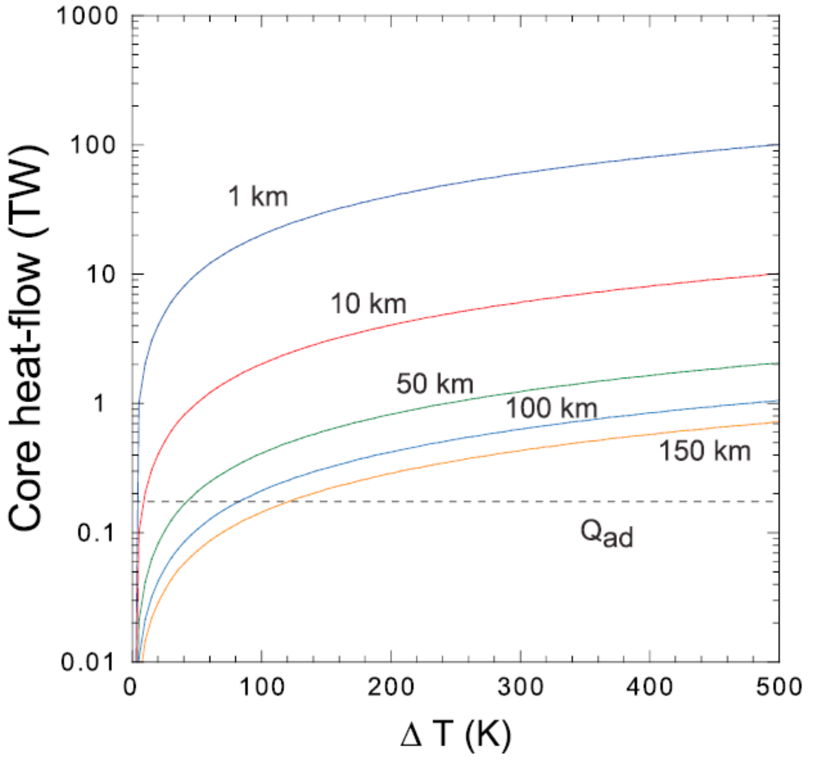

Wiedemann–Franz law

$$\frac{\kappa}{\sigma} = LT$$

Manthilake et al. 2019

Thermal evolution of the planet Mercury

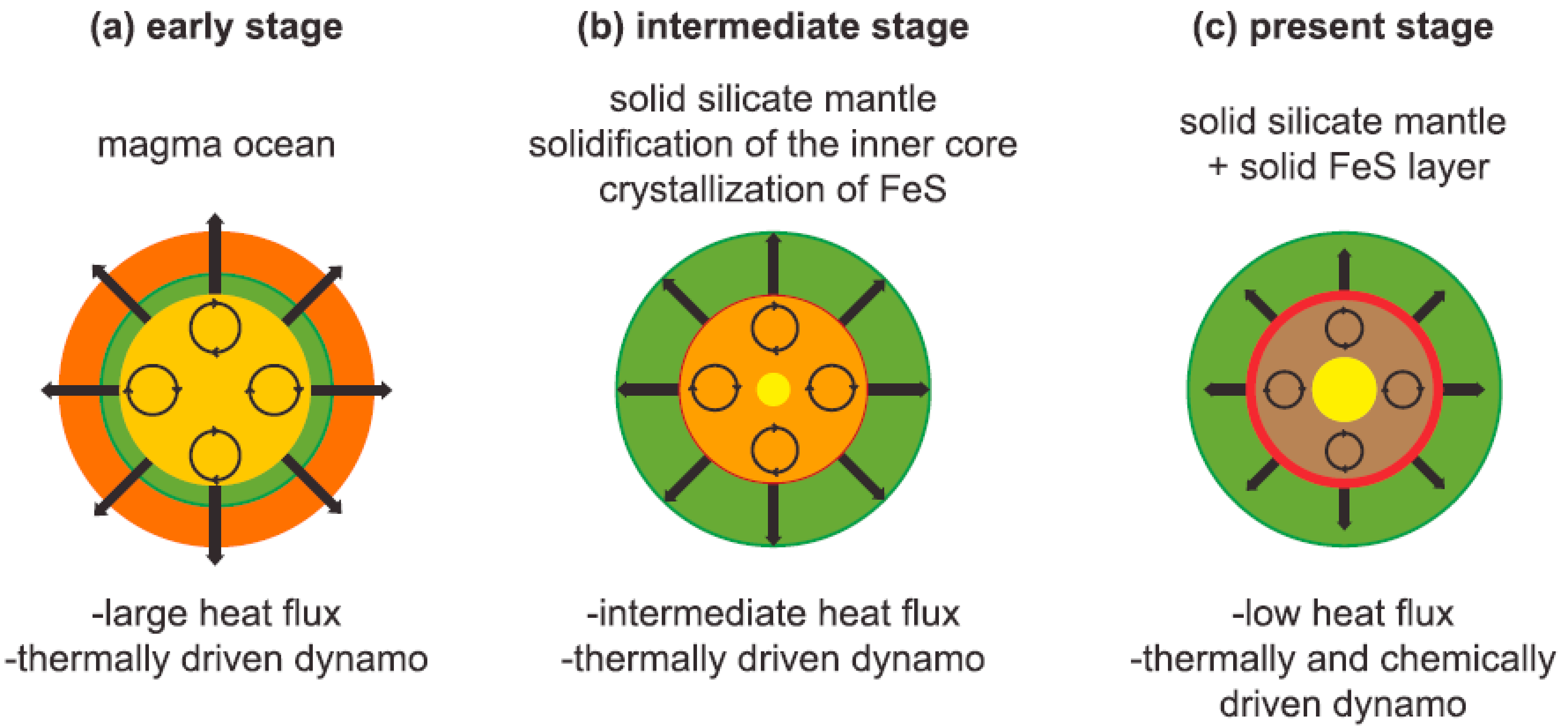

Heat flow is slightly higher than the adiabatic heat flow

Manthilake et al. 2019

Les devises Shadok

IL VAUT MIEUX POMPER MÊME S'IL NE SE PASSE RIEN QUE RISQUER QU'IL SE PASSE QUELQUE CHOSE DE PIRE EN NE POMPANT PAS.